Higher-Order 3D-Shell Elements and Anisotropic 3D Yield Functions for Improved Sheet Metal Forming Simulations: Part II

Alexander Wessel[1,2], Maximilian Schilling[3], Tobias Willmann[3], Alexander Butz[1], Manfred Bischoff[3]

[1]Fraunhofer Institute for Mechanics of Materials IWM,
Woehlerstrasse 11, 79108 Freiburg, Germany
[2]Technical University of Munich, Chair of Metal Forming and Casting,
Walther-Meissner-Strasse 4, 85748 Garching, Germany
[3]University of Stuttgart, Institute for Structural Mechanics,
Pfaffenwaldring 7, 70550 Stuttgart, Germany

Abstract

This two-part series focuses on the industrial application of higher-order 3D-shell elements and anisotropic 3D yield functions in sheet metal forming simulations. In the second part, the effect of plastic anisotropy with respect to the in-plane and out-of-plane behaviour on sheet metal forming simulations is analysed. To this end, parameters of the anisotropic 3D yield function Yld2004-18p were identified by a crystal plasticity modelling approach for an AA6014-T4 aluminium alloy. Different loading conditions related to the plane and full stress state were carried out to study the plastic anisotropy with respect to the in-plane and out-of-plane behaviour. The results of the crystal plasticity simulations were utilised to identify parameters of the Yld2004-18p yield function considering three different data sets. The resulting parameter sets for Yld2004-18p were then applied to a sheet metal forming simulation of a generic car body part. All sheet metal forming simulations were carried out using higher-order 3D-shell elements. The results of this numerical study demonstrate that the plastic anisotropy concerning the in-plane behaviour has a higher relevance than the out-of-plane behaviour for the sheet metal forming process studied. Additionally, the results indicate that setting the parameters of Yld2004-18p associated to the out-of-plane behaviour to their isotropic values is a reasonable assumption for the sheet metal forming process analysed.

1 Introduction

In 2021, Willmann et al. [1] presented a higher-order 3D-shell element to simulate sheet metal forming processes. Compared with the commonly used Reissner-Mindlin shell elements, this higher-order 3D-shell element can account for cross-sectional warping and higher-order strain distributions with respect to the thickness coordinate. The results in Willmann et al. [1] and Schilling et al. [2] demonstrate that this higher-order 3D-shell element can improve the prediction quality of sheet metal forming simulations compared to standard Reissner-Mindlin shell elements. These results are further underlined by the first part of this two-part series, see Schilling et al. [3]. Since this higher-order 3D-shell element takes the full stress state (σ_{11}, σ_{22}, σ_{33}, σ_{23}, σ_{13}, σ_{12}) into account, a three-dimensional constitutive model must be used. With respect to the constitutive model, an anisotropic 3D yield function is usually needed to describe the plastic anisotropy of sheet metals. Various anisotropic 3D yield functions have been proposed in the literature in recent decades. Examples of anisotropic 3D yield functions being available in LS-DYNA are Hill48 [4], Yld91 [5] and Yld2004-18p [6], among others. As anisotropic 3D yield functions are capable of taking the plastic anisotropy related to the out-of-plane behaviour into account, parameters of these yield functions can be distinguished in those representing the plastic anisotropy with respect to the in-plane or out-of-plane behaviour. While parameters associated to the in-plane behaviour are typically identified by experimental results of uniaxial tensile tests in different directions with respect to the rolling direction (RD) or hydraulic bulge tests, parameters describing the out-of-plane anisotropy cannot be determined experimentally. These parameters are typically identified by crystal plasticity simulations. Examples of successfully applied crystal plasticity modelling approaches to identify parameters of anisotropic 3D yield functions can be found in Zhang et al. [7], Zhang et al. [8] and Wessel et al. [9] for instances. However, little attention has been paid to the effect of those parameters on sheet metal forming simulations.

Therefore, this study aims to evaluate the benefits of taking the plastic anisotropy with respect to the in-plane and out-of-plane behaviour into account. For this purpose, parameters of the anisotropic 3D yield function Yld2004-18p are identified by the results of crystal plasticity simulations considering three

different data sets for the parameter identification. Subsequently, the resulting parameter sets for the Yld2004-18p yield function are applied to a sheet metal forming simulation of a generic car body part. As a material, an AA6014-T4 aluminium alloy is considered. All simulations are carried out utilising the recently developed higher-order 3D-shell element presented in Willmann et al. [1].

2   Methods

2.1   Crystal plasticity modelling

The microstructure model used for the investigations in this study was taken from previous work. Detailed information regarding the material characterisation and the microstructure model are given in Wessel et al. [10]. Figure 1 (a) illustrates the microstructure model for the AA6014-T4 aluminium alloy studied. The microstructure model has a cubic geometry with an edge length of 1.0 and was meshed by 64 000 hexahedral elements with linear shape functions. In total, 1000 grains are represented. Each of these 1000 grains is assigned to a crystallographic orientation, which was obtained from a reconstruction of an experimentally obtained orientation density function (ODF) for AA6014-T4. As proposed by Schmidt [11], the microstructure model is constrained by periodic boundary conditions. The rate-dependent crystal plasticity-based constitutive model used for the microstructure model is based on the work of Asaro [12] together with the numerical framework presented in Kalidindi et al. [13]. In accordance with Lebensohn et al. [14], the hardening is described by an extended Voce-type hardening law following Tomé et al. [15]. Further information regarding the crystal plasticity-based constitutive model and its implementation are given in Pagenkopf [16]. Parameters of the crystal plasticity model were identified by a reverse engineering approach to fit the experimental stress-strain curve at 0° with respect to RD as shown in Figure 1 (b).

(a)

(b)
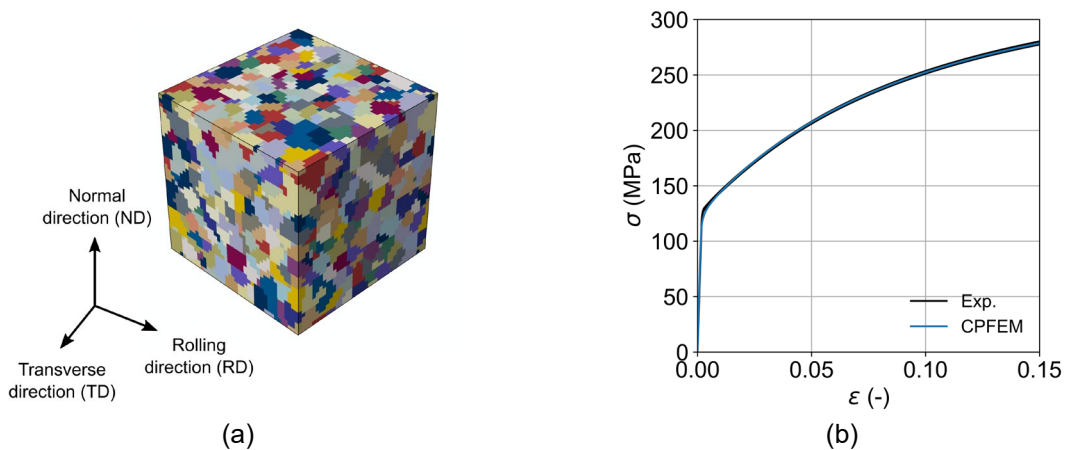
Fig.1:   *(a) Microstructure model representing AA6014-T4 aluminium alloy and (b) experimental stress-strain curve in comparison with the results of the crystal plasticity simulation. Parameters of the crystal plasticity-based constitutive model were adjusted to match the experimental stress-strain curve. Figures are taken from Wessel et al. [10].*

The results for the normalised yield stresses as well as the r-values at 15°, 30°, 45°, 60°, 75° and 90° with respect to RD in Figure 2 show that the r-values are predicted with high accuracy. Differences regarding the experimental normalised yield stresses are highest at 45° with respect to RD and account for 4.18%. These differences were already discussed in Wessel et al. [10] and are most likely caused by precipitate related effects.
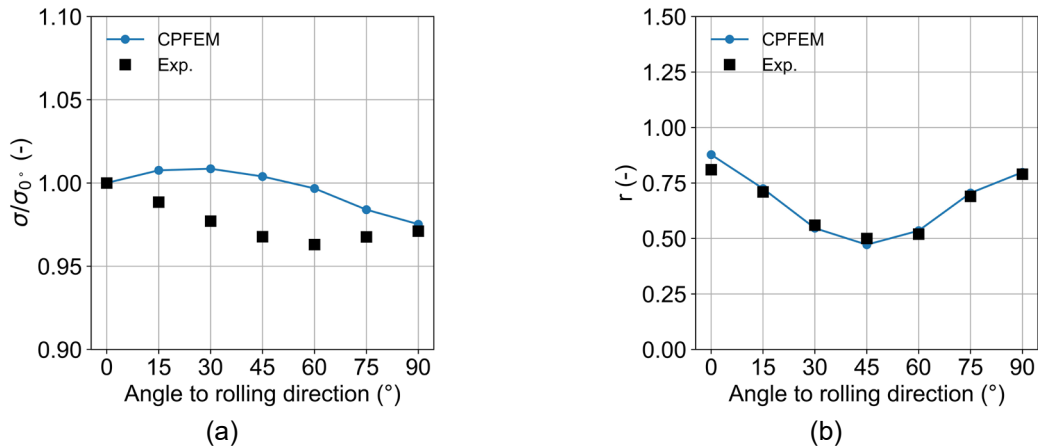
Fig.2: (a) Normalised yield stress and (b) r-value as predicted by crystal plasticity simulations in comparison with experimental data. Figures are taken from Wessel et al. [10].

To explore the anisotropic 3D yield surface using crystal plasticity simulations or rather virtual experiments, 300 crystal plasticity simulations were carried out. Of these 300 crystal plasticity simulations, 100 were sampled with respect to the plane stress state (σ_{11}, σ_{22}, σ_{12}) following a machine learning based sampling approach presented in Wessel et al. [17]. This approach uses the machine learning technique active learning to explore the anisotropic yield surface by means of crystal plasticity simulations in a data efficient manner. Regarding the out-of-plane behaviour, 200 additional crystal plasticity simulations were performed following the extension of the machine learning based sampling approach with respect to the full stress state, see Wessel et al. [9]. To determine the points on the yield surface, all virtual experiments were post-processed considering a specific plastic work of 15.49 MPa. This corresponds to a true plastic strain of 0.08 in RD. The resulting points on the yield surface were then used to identify parameters of the Yld2004-18p yield function using the least-squares method. As proposed by van den Boogaard et al. [18], the parameters c'_{12} and c'_{13} were set to unity and, hence, the number of independent parameters associated to the in-plane behaviour reduces to 12. The following three data sets were used to identify three different parameter sets for Yld2004-18p:

1. **Yld2004-18p (Set 1):** The in-plane parameters of Yld2004-18p were identified based on the crystal plasticity simulations of the uniaxial tensile tests at 0°, 15°, 30°, 45°, 60°, 75° and 90° with respect to RD in Figure 2. Both, the normalised yield stresses identified at a specific plastic work of 15.49 MPa as well as the r-values determined between 0.1 and 0.175 true plastic strain were utilised to identify the parameters of the anisotropic 3D yield function.
2. **Yld2004-18p (Set 2):** All 300 crystal plasticity simulations, or rather the corresponding points on the yield surface, were utilised to determine the in-plane and out-of-plane parameters of Yld2004-18p. Subsequently, parameters associated to the out-of-plane behaviour were set to unity, which corresponds to the isotropic value.
3. **Yld2004-18p (Set 3):** Similar to Yld2004-18p (Set 2), all 300 crystal plasticity simulations are used to determine all parameters for the Yld2004-18p yield function. As a result, Yld2004-18p (Set 2) and Yld2004-18p (Set 3) share the same 12 parameters associated to the in-plane behaviour. In contrast to the first two parameter sets, Yld2004-18p (Set 1) and Yld2004-18p (Set 2), parameters describing the out-of-plane behaviour are not set to the isotropic values and, hence, the plastic anisotropy with respect to the out-of-plane behaviour is taken into account.

The purpose of the three different parameter sets for the Yld2004-18p yield function is to study the effect of the plastic anisotropy with respect to the in-plane and out-of-plane behaviour. While the comparison of Yld2004-18p (Set 1) and Yld2004-18p (Set 2) focuses on the effect of the plastic anisotropy with respect to the in-plane behaviour, Yld2004-18p (Set 2) and Yld2004-18p (Set 3) are compared to analyse the effect of parameters associated to the out-of-plane behaviour.

2.2   Sheet metal forming simulations

For analysing the three parameter sets for the Yld2004-18p yield function, the BMW test model RWU-80 was examined. This test model was designed by Katy Hammer from BMW Group and represents typical features of a sheet metal forming simulation of car body parts, see Figure 3. Further details of

this generic car body part are given in Fleischer et al. [19]. In the forming simulation for this generic car body part a blank is clamped between a die and a blankholder – both having a drawbead. Then, the blank is formed into its final shape by a punch. No trimming operation or springback is considered in the forming simulation.
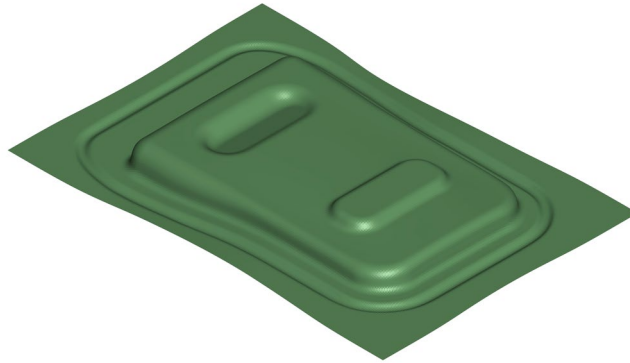
Fig.3: Geometry of the generic car body part utilised for analysing the effect of plastic anisotropy with respect to the in-plane and out-of-plane behaviour.

The blank has a thickness of 1.16 mm and was meshed by about 50 000 four-node shell elements. Here, the recent higher-order 3D-shell elements presented in Willmann et al. [1] were applied via a developer version of the commercial Finite Elements Software LS-DYNA. Tools were meshed by Belytschko-Tsay shell elements (ELFORM=2) and considered to be rigid. All simulations were performed using an explicit time integration scheme.

3   Results

3.1   Crystal plasticity simulations

Results of the 100 crystal plasticity simulations considering a plane stress state are illustrated in Figure 4. Each marker represents one point on the yield surface for the AA6014-T4 aluminium alloy. Further, the 200 crystal plasticity simulations considering a full stress state were analysed at the same specific plastic work of 15.49 MPa. As the resulting points on the yield surface are six-dimensional, the data cannot be visualised reasonably.
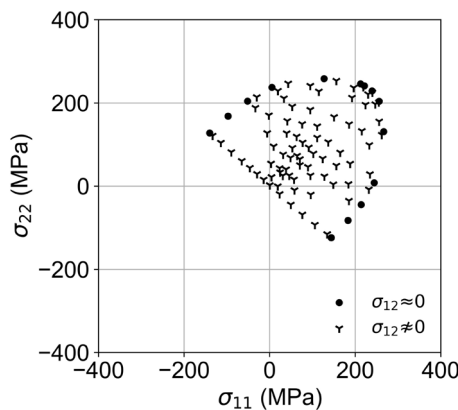
Fig.4: Points on the yield surface determined by 100 crystal plasticity simulations for the plane stress state. Each point was determined considering a specific plastic work of 15.49 MPa.

3.2   Anisotropic yield surfaces

Based on the results of the crystal plasticity simulations in Section 3.1, the three parameter sets for the Yld2004-18p yield function were identified as described in Section 2.1. The comparison of the resulting yield surfaces in Figure 5 illustrates that there are differences in the in-plane anisotropy between Yld2004-18p (Set 1) and Yld2004-18p (Set 2). The yield surface for the parameter set Yld2004-18p

(Set 1) shows a higher deviation regarding the yield points in the biaxial/plain strain area compared to Yld2004-18p (Set 2) as shown in Figure 5 (a). Besides the biaxial and the plane strain area, there are also differences in the simple shear area, see Figure 5 (b). For Yld2004-18p (Set 1), the normalised yield stress $\sigma_{12}/\sigma_{0°}$ for simple shear amounts to 0.58, while the corresponding value for Yld2004-18p (Set 2) amounts to 0.61.
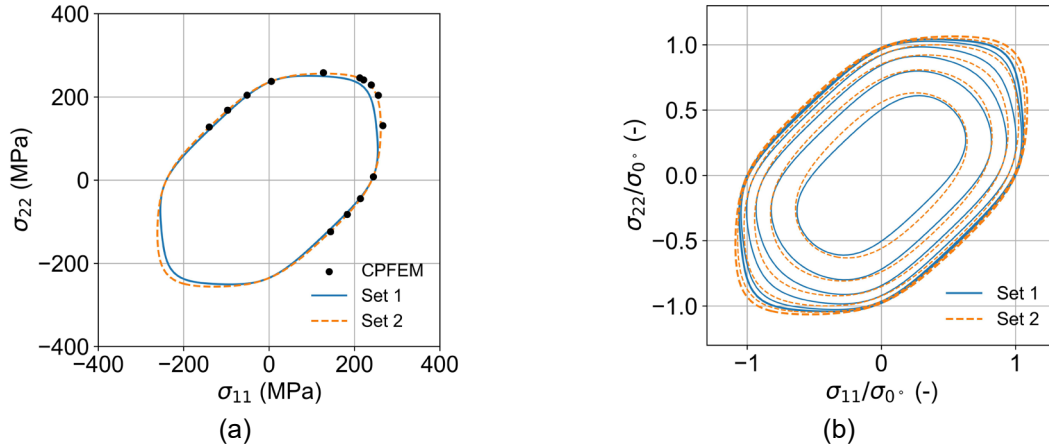
Fig.5: (a) Comparison of the Yld2004-18p yield surfaces for the parameter sets Yld2004-18p (Set 1) and Yld2004-18p (Set 2). Only yield points with $\sigma_{12} \approx 0$ are illustrated. (b) Normalised yield surfaces for the first and second parameter set of the Yld2004-18p yield function. Normalised shear contours are shown in increments of 0.1 from 0.0 to 0.5.

Figure 6 compares the normalised yield stresses and the r-values with respect to RD for Yld2004-18p (Set 1) and Yld2004-18p (Set 2). Here, both parameter sets for Yld2004-18p show a good match with the crystal plasticity simulations of the uniaxial tensile tests at 0°, 15°, 30°, 45°, 60°, 75° and 90° with respect to RD. For Yld2004-18p (Set 1) the agreement is slightly better.
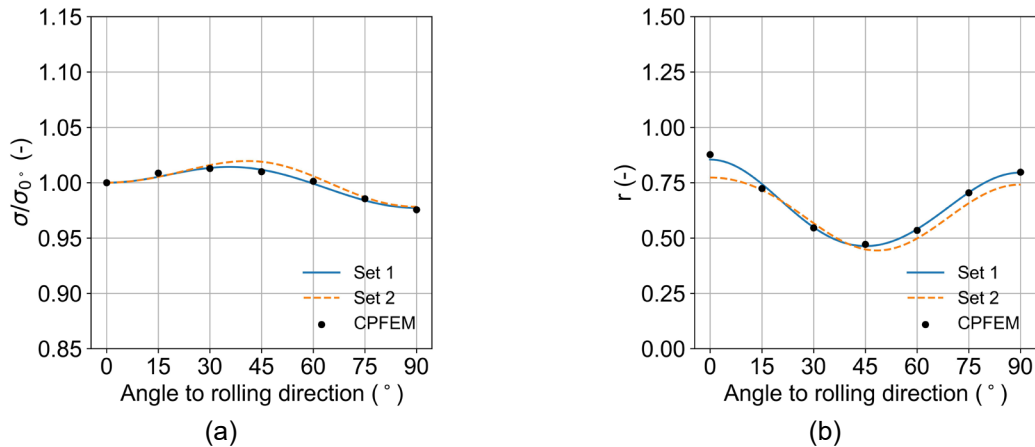
Fig.6: (a) Normalised yield stresses and (b) r-values with respect to RD for Yld2004-18p (Set 1) and Yld2004-18p (Set 2).

As idented by the data sets, the anisotropic yield surfaces for Yld2004-18p (Set 2) and Yld2004-18p (Set 3) in Figure 7 (a) show an identical anisotropic yield surface with respect to the in-plane behaviour. Differences occur regarding the out-of-plane behaviour and, in particular, with respect to the shear stresses σ_{23} and σ_{13} as shown in Figure 7 (b) and (c), respectively. The normalised simple shear stress $\sigma_{23}/\sigma_{0°}$ for Yld2004-18p (Set 2) in Figure 7 (b) is 0.54 compared to 0.61 for Yld2004-18p (Set 3). The values for the normalised simple shear stress $\sigma_{13}/\sigma_{0°}$ for Yld2004-18p (Set 2) and Yld2004-18p (Set 3) in Figure 7 (c) also amount to 0.54 and 0.61, respectively.
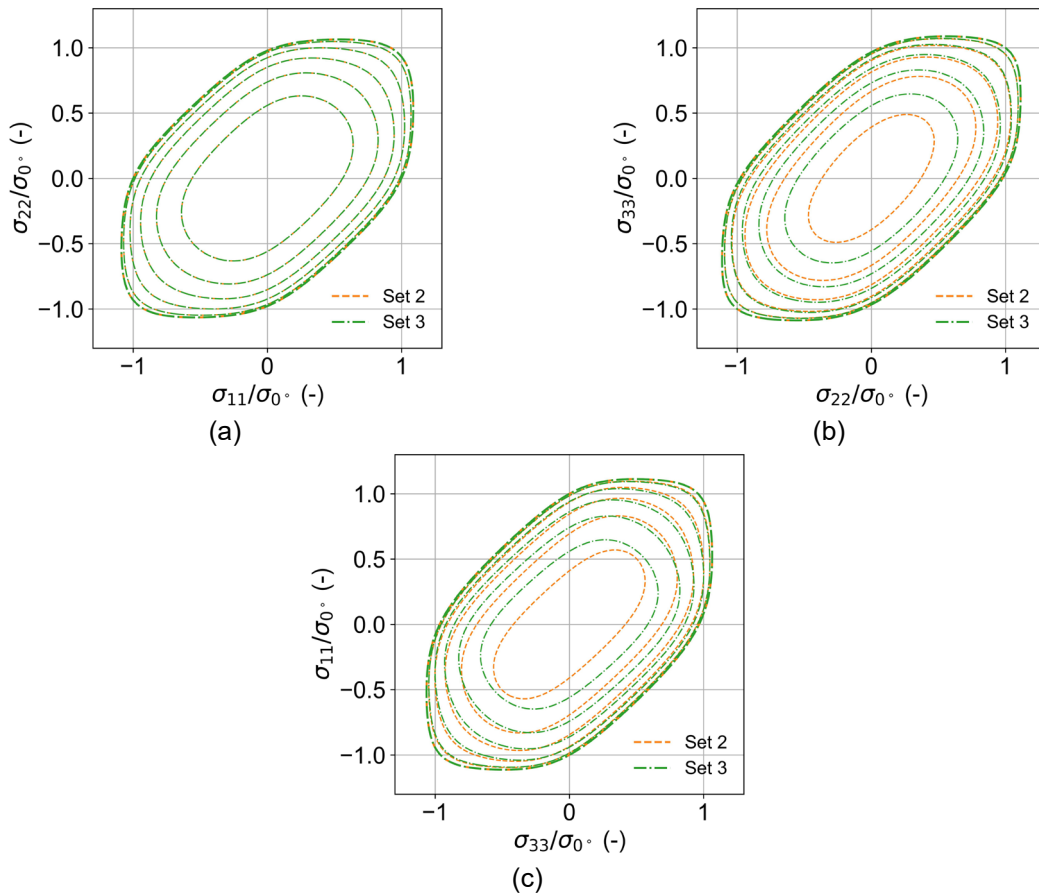
Fig.7: *Normalised yield surface with respect to (a) the σ_{11}-σ_{22} plane, (b) the σ_{22}-σ_{33} plane, (c) the σ_{33}-σ_{11} plane for the second and third parameter set of the Yld2004-18p yield function. Normalised shear contours are shown in increments of 0.1 from 0.0 to 0.5.*

3.3 Forming simulation of a car body part

The results of the sheet metal forming simulation for the generic car body part are shown in Figure 8 considering the von-Mises stress. Overall, the stress fields for the three parameter sets of the Yld2004-18p yield function are comparable. Differences occur primarily between the results of Yld2004-18p (Set 1) and Yld2004-18p (Set 2/Set 3). In this respect, Yld2004-18p (Set 2) and Yld2004-18p (Set 3) predict slightly higher von Mises stresses in comparison to Yld2004-18p (Set 1). The results for the von-Mises stress for the second and third parameter set are nearly identical.
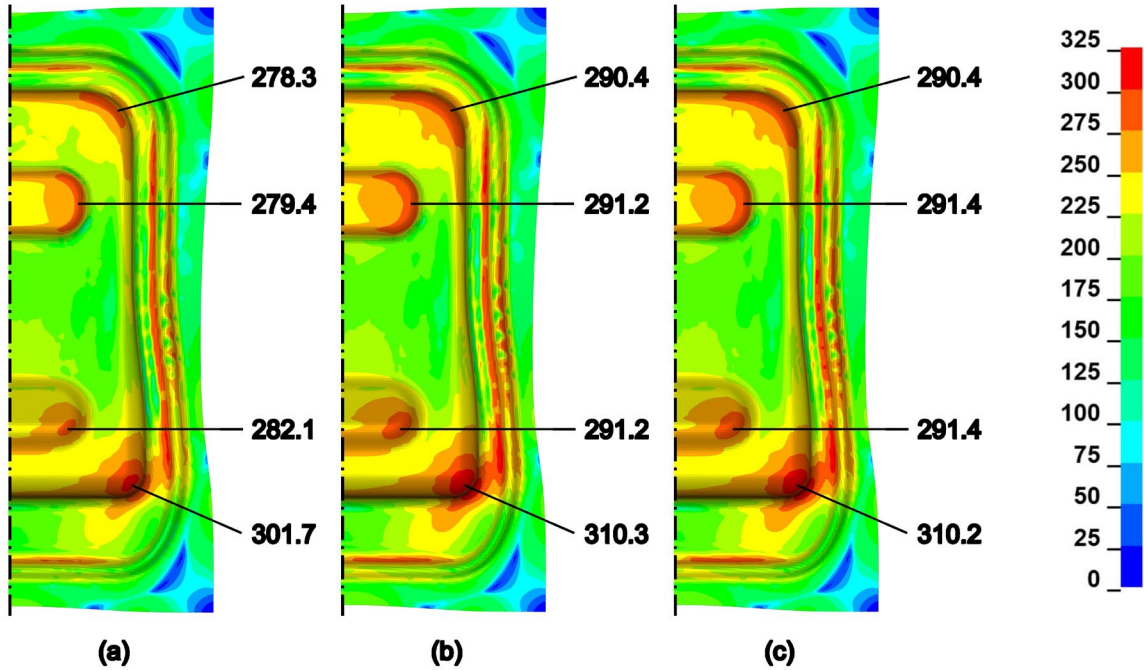
Fig.8: *Von-Mises stress given in MPa as evaluated at the outer shell surface for (a) Yld2004-18p (Set 1), (b) Yld2004-18p (Set 2) and (c) Yld2004-18p (Set 3). Due to symmetry, only half of the generic car body part is illustrated.*

Figure 9 illustrates the results for the effective plastic strain. Again, differences are visible primarily between Yld2004-18p (Set 1) and Yld2004-18p (Set 2/Set 3). The maximum effective plastic strain of the first variant amounts to 0.36. This is about 9.1% higher than the corresponding results for the second and third parameter set for Yld2004-18p, which are nearly the same.
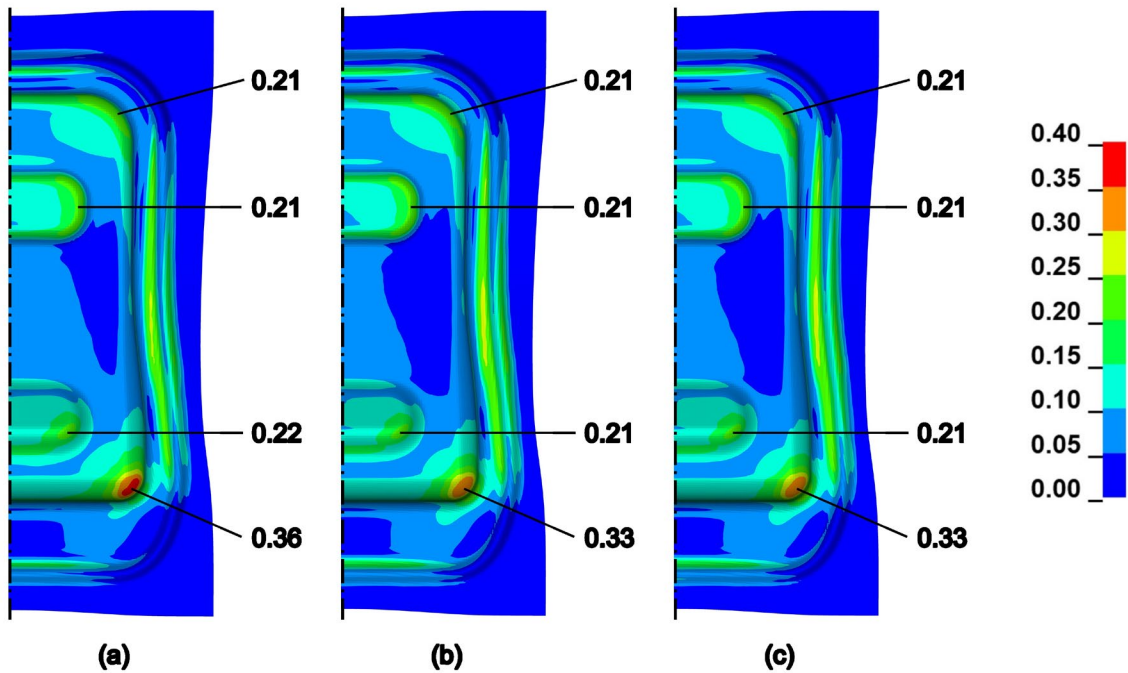
Fig.9: *Effective plastic strain as evaluated at the outer shell surface for (a) Yld2004-18p (Set 1), (b) Yld2004-18p (Set 2) and (c) Yld2004-18p (Set 3). Due to symmetry, only half of the generic car body part is illustrated.*

4 Discussion

The results of this study demonstrate that the higher-order 3D-shell element presented in Willmann et al. [1] can be successfully combined with anisotropic 3D yield functions like Yld2004-18p to simulate large industry-orientated sheet metal forming processes. Furthermore, the results in Section 3 indicate the following three aspects regarding the use of anisotropic 3D yield models: Firstly, as expected, the results of the crystal plasticity simulations in Section 3.2 demonstrate that different data sets affect the parameter identification of anisotropic yield functions or rather the resulting yield surfaces. Parameters for the first parameter set of the Yld2004-18p yield function were identified based on the crystal plasticity results of seven uniaxial tensile tests, while for the second parameter set 300 crystal plasticity simulations were considered. As in both cases, data for the uniaxial stress state or the area close to the uniaxial stress state were taken into account for the parameter identification, Yld2004-18p (Set 1) and Yld2004-18p (Set 2) show comparable results for the normalised yield stresses and r-values in Figure 6. Since Yld2004-18p (Set 1) was directly fitted to the points of the uniaxial tensile tests, the error is slightly lower compared to Yld2004-18p (Set 2). By contrast, for non-uniaxial stress states the differences in the yield surface between Yld2004-18p (Set 1) and Yld2004-18p (Set 2) can be explained by the missing data points in the plane strain and biaxial area of the first data set. This example nicely underlines the importance of considering data from various stress states for the parameter identification of anisotropic yield models. Assuming that the microstructure model captures the anisotropic plastic material behaviour of sheet metal with sufficient accuracy, crystal plasticity simulations can provide additional information to improve the parameter identification of anisotropic yield functions, particularly in areas that cannot be analysed experimentally.

Secondly, the results in Section 3.3 show the implications of these data sets or rather the resulting differences in the yield surfaces on a sheet metal forming simulation. From the results of the sheet metal forming simulation in Figure 8 and Figure 9 follows that the plastic anisotropy with respect to the in-plane behaviour has a higher relevance than the out-of-plane behaviour for the generic car body part studied. For the von-Mises stress, the difference between Yld2004-18p (Set 1) and Yld2004-18p (Set 2/Set 3) may not seem very high, too. However, these differences in the stresses might lead to more pronounced differences in a subsequent springback simulation, which was not taken into account.

Finally, as the results of the forming simulations for the second and third parameter set for the Yld2004-18p yield function in Figure 8 and Figure 9 are nearly identical, it can be concluded that the assumption of setting the parameters associated to the out-of-plane behaviour to their isotropic values is a reasonable approach for the forming process of the AA6014-T4 aluminium sheet studied. This assumption is expected to be also reasonable for other sheet metal forming simulations being comparable. On the other hand, the plastic anisotropy with respect to the out-of-plane behaviour might be relevant for sheet metal forming processes with more pronounced shear stresses σ_{23} and σ_{13} like single point incremental forming. For example, Esmaeilpour et al. [20] considered the plastic anisotropy with respect to the out-of-plane behaviour to simulate the single point incremental forming process of a conical sheet part made out of AA7075-O aluminium alloy.

5 Summary

This study utilised higher-order 3D-shell elements to simulate the sheet metal forming process of a generic car body part and analysed the effect of taking the plastic anisotropy with respect to the out-of-plane behaviour into account. Thus, parameters of the anisotropic 3D yield function Yld2004-18p were identified by crystal plasticity simulations considering three different data sets. In summary, the following conclusions can be drawn from the present work:

- The higher-order 3D-shell element presented in Willmann et al. [1] can be successfully applied in combination with anisotropic 3D yield functions like Yld2004-18p to simulate industry-orientated sheet metal forming processes such as the generic car body part.
- The data used for the parameter identification of anisotropic yield functions affect the resulting yield surfaces. Here, crystal plasticity simulations can provide additional information to improve the accuracy of the parameter identification for anisotropic yield functions.
- For the generic car body part analysed, the plastic anisotropy with respect to the in-plane behaviour had a higher relevance than the out-of-plane behaviour. As the effect of the latter was neglectable, setting the parameters associated to the out-of-plane behaviour to their isotropic values is considered a reasonable approach for the forming process studied.

6   Acknowledgement

7   Literature

[1]   Willmann, T., Wessel, A., Beier, T., Butz, A., Bischoff, M.: "Cross-Sectional Warping in Sheet Metal Forming Simulations", 13th European LS-DYNA Conference, 2021.

[2]   Schilling, M., Willmann, T., Bischoff, M.: "3D-Shell Elements for Improved Prediction Quality in Sheet Metal Forming Simulations", 16th LS-DYNA Forum, 2022.

[3]   Schilling, M., Willmann, T., Wessel, A., Butz, A., Bischoff, M.: "Higher-Order 3D-Shell Elements and Anisotropic 3D Yield Functions for Improved Sheet Metal Forming Simulations: Part I", 14th European LS-DYNA Conference, 2023.

[4]   Hill, R.: "A theory of the yielding and plastic flow of anisotropic metals", Proceedings of the Royal Society of London. Series A. Mathematical and Physical Sciences, 193.1033, 1948, 281-297.

[5]   Barlat, F., Lege, D. J., Brem, J. C.: "A six-component yield function for anisotropic materials", International Journal of Plasticity, 7, 1991, 693-712.

[6]   Barlat, F., Aretz, H., Yoon, J. W., Karabin, M., Brem, J. C., Dick, R.: "Linear transfomation-based anisotropic yield functions", International Journal of Plasticity, 21, 2005, 1009-1039.

[7]   Zhang, K., Holmedal, B., Hopperstad, O. S., Dumoulin, S., Gawad, J., Van Bael, A., Van Houtte, P.: "Multi-level modelling of mechanical anisotropy of commercial pure aluminium plate: crystal plasticity models, advanced yield functions and parameter identification", International Journal of Plasticity, 66, 2015, 3-30.

[8]   Zhang, H., Diehl, M., Roters, F., Raabe, D.: "A virtual laboratory using high resolution crystal plasticity simulations to determine the initial yield surface for sheet metal forming operations", International Journal of Plasticity, 80, 2016, 111-138.

[9]   Wessel, A., Morand, L., Butz, A., Helm, D., Volk, W.: "Machine learning-based sampling of virtual experiments within the full stress state to identify parameters of anisotropic yield models", arXiv preprint arXiv:2211.00090, 2022.

[10]   Wessel, A., Perdahcioğlu, E. S., Butz, A., van den Boogaard, T., Volk, W.: "Prediction of texture-induced plastic anisotropy in AA6014-T4 aluminium sheets utilising two different crystal plasticity-based constitutive models", IOP Conference Series: Materials Science and Engineering, IOP Publishing, 2023, p. 012059.

[11]   Schmidt, I.: "Numerical homogenisation of an elasto-plastic model-material with large elastic strains: macroscopic yield surfaces and the Eulerian normality rule", Computational Mechanics, 48, 2011, 579-590.

[12]   Asaro, R. J.: "Micromechanics of crystals and polycrystals", Advances in Applied Mechanics, 23, 1983, 1-115.

[13]   Kalidindi, S. R., Bronkhorst, C. A., Anand, L.: "Crystallographic texture evolution in bulk deformation processing of FCC metals", Journal of the Mechanics and Physics of Solids, 40, 1992, 537-569.

[14]   Lebensohn, R. A., Tomé, C. N., Castaneda, P. P.: "Self-consistent modelling of the mechanical behaviour of viscoplastic polycrystals incorporating intragranular field fluctuations", Philosophical Magazine, 87, 2007, 4287-4322.

[15]   Tome, C., Canova, G. R., Kocks, U. F., Christodoulou, N., Jonas, J. J.: "The relation between macroscopic and microscopic strain hardening in FCC polycrystals", Acta Metallurgica, 32, 1984, 1637-1653.

[16]   Pagenkopf, J.: "Bestimmung der plastischen Anisotropie von Blechwerkstoffen durch ortsaufgelöste Simulationen auf Gefügeebene", Fraunhofer Verlag, 2018.

[17]   Wessel, A., Morand, L., Butz, A., Helm, D., Volk, W.: "A new machine learning based method for sampling virtual experiments and its effect on the parameter identification for anisotropic yield models", IOP Conference Series: Materials Science and Engineering, IOP Publishing, 2021, p. 012026.

[18] van den Boogaard, T., Havinga, J., Belin, A., Barlat, F.: "Parameter reduction for the Yld2004-18p yield criterion", International Journal of Material Forming, 9, 2016, 175-178.

[19] Fleischer, M., Sitz, S., Asen, F., Craighero, P., Paramasivam, N.: "Simulation of Sheet Metal Forming – Current Developments", 16th LS-DYNA Forum, 2022.

[20] Esmaeilpour, R., Kim, H., Park, T., Pourboghrat, F., Xu, Z., Mohammed, B., Abu-Farha, F.: "Calibration of Barlat Yld2004-18P yield function using CPFEM and 3D RVE for the simulation of single point incremental forming (SPIF) of 7075-O aluminum sheet", International Journal of Mechanical Sciences, 145, 2018, 24-41.